



Published in final edited form as:

ChemMedChem. 2019 November 06; 14(21): 1863–1872. doi:10.1002/cmdc.201900508.

Potent HIV-1 Protease Inhibitors Containing Carboxylic and Boronic Acids: Effect on Enzyme Inhibition and Antiviral Activity and Protein-ligand X-ray Structural Studies

Arun K. Ghosh^a, Zilei Xia^a, Satish Kovala^a, William L. Robinson^a, Megan E. Johnson^a, Daniel W. Kneller^b, Yuan-Fang Wang^b, Manabu Aoki^{d,e}, Yuki Takamatsu^e, Irene T. Weber^b, Hiroaki Mitsuya^{c,d,e}

^[a]Department of Chemistry and Department of Medicinal Chemistry, Purdue University, West Lafayette, IN 47907,

^[b]Departments of Biology and Chemistry, Molecular Basis of Disease, Georgia State University, Atlanta, GA 30303

^[c]Departments of Hematology and Infectious Diseases, Kumamoto University School of Medicine, Kumamoto 860-8556, Japan

^[d]Experimental Retrovirology Section, HIV and AIDS Malignancy, Branch, National Cancer Institute, Bethesda, MD 20892

^[e]Department of Refractory Viral Infections, National Center for Global Health and Medicine Research Institute, Shinjuku, Tokyo 162-8655, Japan

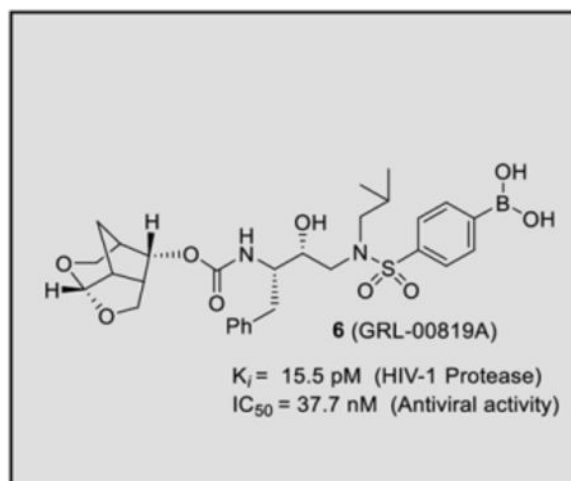
Abstract

We report here the synthesis and biological evaluation of phenylcarboxylic acid and phenylboronic acid containing HIV-1 protease inhibitors and their functional effect on enzyme inhibition and antiviral activity in MT-2 cell lines. Inhibitors bearing *bis*-THF ligand as P2 ligand and phenylcarboxylic acids and carboxamide as the P2' ligands, showed very potent HIV-1 protease inhibitory activity. However, carboxylic acid containing inhibitors showed very poor antiviral activity compared to carboxamide-derived inhibitors which showed good antiviral IC₅₀ value. Boronic acid-derived inhibitor with *bis*-THF as the P2 ligand showed very potent enzyme inhibitory activity, but it showed relatively reduced antiviral activity compared to darunavir in the same assay. Boronic acid-containing inhibitor with a P2-*Cm*-THF ligand also showed potent enzyme K_i but significantly reduced antiviral activity. We have evaluated antiviral activity against a panel of highly drug-resistant HIV-1 variants. One of the inhibitors maintained good antiviral activity against HIV_{DRV}^R_{P20} and HIV_{DRV}^R_{P30} viruses. We have determined high resolution X-ray structures of two synthetic inhibitors bound to HIV-1 protease and obtained molecular insight into the ligand-binding site interactions.

Graphical Abstract

akghosh@purdue.edu.

Supporting information for this article is given via a link at the end of the document.



We report structure-based design, synthesis, biological evaluation and X-ray structural studies of a series of exceptionally potent HIV-1 protease inhibitors containing boronic acid-based P2' – ligands to interact with active site residues in the S2'-subsite.

Keywords

HIV-1 protease inhibitors; brain penetration; Drug resistance; dimerization inhibitor; Structure-based design; synthesis; genetic barrier

Introduction

Structure-based molecular design has become one of the most successful and widely used strategies for preclinical drug development. Over the years, it has led to numerous first-in-class approved drugs and preclinical candidates.^{1,2} Structure-based design strategies have played a key role in the design and development of HIV-1 protease inhibitor drugs.^{3,4} HIV-1 protease inhibitors are an important component of current antiretroviral therapy (ART) which is responsible for dramatic improvement of life expectancy and mortality rates of HIV/AIDS patients in the developing nations. HIV-1 protease is an aspartic acid protease which plays a critical role in viral replication.^{5,6} HIV-1 protease inhibitor (PI) drugs block HIV-1 protease and generate morphologically immature and noninfectious virions.^{7,8} Darunavir (**1**, Figure 1), the latest FDA-approved PI, has been highly efficacious in suppressing HIV-1 replication and showing significant clinical benefits to HIV/AIDS patients.^{9,10} Darunavir has emerged as a widely used first-line therapy for rescue treatment.^{11,12} Its exceptional resistance profile is due to a dual mechanism of action as it inhibits HIV-1 protease and inhibits dimerization of HIV-1 protease monomers.¹³

Darunavir was developed by structure-based design strategies with particular emphasis on maximizing active site interactions, especially promoting strong hydrogen bonding interactions with the HIV-1 backbone atoms in the S2 and S2' subsites.^{14,15} In this context, we created a stereochemically defined 3(*R*),6*a*(*R*)-bis-tetrahydrofuranyl urethane as the P2 ligand to form hydrogen bonds with the Asp29 and Asp30 backbone NHs in the S2-subsite.

Also, the P2'–4-aminobenzene sulfonamide was incorporated to interact with the backbone atoms in the S2' subsite.^{16,17} These inhibitor design strategies targeting the protein backbone may be responsible for darunavir's exceptional antiviral activity against highly multidrug-resistant HIV-1 variants.^{18,19} However, DRV-resistant HIV-1 variants have emerged, and development of novel antiviral drugs with a high genetic barrier against multidrug-resistant HIV-1 variants including DRV-resistant variants is urgently needed.^{20,21} In this context, we investigated further optimization of structural elements of darunavir that would enhance backbone interactions in the active site of HIV-1 protease.

The X-ray structure of darunavir-bound HIV-1 protease [PDB 1D : 4HLA] revealed that the P2' 4-aminosulfonamide ligand is involved in water-mediated hydrogen bonding interactions with Gly48' backbone amide NH through two crystallographic water molecules.^{17,22} Based upon this observation, we speculated that the modification of amine functionality with a carboxylic acid or with a carboxamide group would replace one of these two crystallographic water molecules closer to the amine functionality. Such modified ligands could not only maintain strong hydrogen bonds with backbone NH of Asp30, but also the carboxylic acid derivative can form a water-mediated hydrogen bond with the Gly48' NH located in flap region of HIV-1 protease. Indeed, the resulting modified inhibitors **3** and **4** exhibited very potent enzyme inhibitory activity with K_i values of 12.9 pM and 8.9 pM, respectively.²² Interestingly, carboxylic acid-derived inhibitor **3** did not exhibit any appreciable antiviral activity in MT-2 cells. However, inhibitor **4** with a carboxamide derivative showed antiviral IC_{50} value of 93 nM in MT-2 cells.²² This result is not surprising as it has been reported that intracellular concentration of PIs are a dynamic balance between influx, efflux, and sequestration.^{23,24} Since DRV has been shown to serve as a transport substrate of P-glycoprotein, the carboxylic acid derivatives are expected to show similar efflux profiles.²⁵ Thus, we have assayed intracellular concentrations of inhibitor **3** and **4** in MT-2 and MT-4 cells. Interestingly, both cell lines showed very low uptake of carboxylic acid-derived inhibitor **3**.²² The sequestration and influx properties of PIs are important issues that need serious attention for PI design. We have determined X-ray crystal structures of inhibitor **3** and **4** with HIV-1 protease complexes. Our structural analysis revealed enhanced hydrogen bonding interactions in the S2' subsite compared to DRV-HIV-1 protease complex.²² A stereoview of the active site interactions of inhibitor-bound HIV-1 protease is shown in Figure 2. As can be seen, the P2' 4-carboxylic acid ligand is involved in water-mediated hydrogen bonding interactions with Gly48' backbone amide NH located in the flap region of HIV-1 protease.^{17,22} More recently, Raines and co-workers reported the HIV-1 protease inhibitor **5** with a phenyl boronic acid as the P2' ligand.²⁶ This inhibitor also exhibited very potent enzyme inhibitory activity compared to darunavir. Furthermore, X-ray crystal structure of inhibitor **5**-bound HIV-1 protease revealed that boronic acid is involved in enhanced hydrogen bonding interaction including a water-mediated hydrogen bonding interaction with Gly48' similar to inhibitor **3** and **4**.²⁶ While boronic acid containing inhibitor **5** displayed potent enzyme inhibitory activity, assessment of its antiviral activity in cell-based assays was not carried out. Thus, the intriguing question is whether boronic acid-derived inhibitors show better antiviral potency compared to carboxylic acid-derived compounds. In the present studies, we have synthesized a selected group of HIV-1 protease inhibitors containing boronic acid as the P2' ligand and evaluated their enzyme inhibitory

activity as well as antiviral activity compared to darunavir. Furthermore, we have evaluated antiviral activity against a panel of highly darunavir-resistant HIV-1 variants for compounds **5** and **6** with darunavir control. To assess ligand-binding site interactions, we have determined a high resolution X-ray structure of inhibitor **6**-bound HIV-1 protease.

Synthesis of carboxylic and boronic acid-based inhibitors

For our investigation regarding the effect on enzyme inhibitory and antiviral activity for inhibitors containing 4-phenylcarboxylic acid and 4-phenylboronic acid as the P2' ligand, we have synthesized a set of selected inhibitors. The synthesis of 4-phenylcarboxylic acid derivatives **11** and **13** is shown in Scheme 1. Commercially available (*S,S*)-3(*t*-Boc-amino)-1,2-epoxy-4-phenylbutane **7** was converted to hydroxyethylamine sulfonamide derivative **8** with a diacetoxymethyl group as P2' ligand as described by us previously.²⁷ Exposure of the acetate derivative **8** to K₂CO₃ in methanol at 23 °C for 30 min provided the corresponding aldehyde. Pinnick oxidation²⁸ of the resulting aldehyde with sodium chlorite in *t*-butanol in the presence of 2-methyl-2-butene and phosphate buffer afforded the carboxylic acid derivative **9** in 86% yield over 2-steps. For the conversion of carboxylic acid derivative **9** to inhibitor **11** Boc-group was removed by exposure to trifluoroacetic acid (TFA) in CH₂Cl₂ at 0 °C to 23 °C for 3 h. Reaction of the resulting amine with known²⁹ activated carbonate of tetrahydropyranofuran **10** in the presence of diisopropylethylamine (DIPEA) in CH₃CN at 23 °C for 10 d afforded inhibitor **11** in 37% yield over 2-steps. For the synthesis of carboxylic acid derivative **13**, Boc derivative **9** was treated with TFA and the resulting amine was reacted with *crown*-THF carbonate **12**³⁰ as described above to provide **13** in 80% yield over 2 steps.

For convenient synthesis of inhibitors containing 4-phenylboronic acid, we first prepared 4-(chlorosulfonyl)-phenyl boronic acid. As shown in Scheme 2, commercially available 4-bromophenyl sulfonyl chloride **14** was treated with NaOMe in methanol at 0 °C to 23 °C for 12 h to provide the corresponding methyl sulfonate derivative in 62% yield.³¹ Reaction of the resulting 4-bromosulfonate derivative with *n*BuLi in THF at -78 °C for 10 min followed by addition of B(OMe)₃ at -78 °C for 20 min provided boronic acid derivative **15** in 45% yield. Treatment of **15** with triethylamine in methanol 60 °C for 24 h followed by reaction of the resulting triethylammonium salt with thionyl chloride, heated at 80 °C for 24 h furnished, sulfonyl chloride **16** in 89% yield.³² This sulfonyl chloride was then reacted with the known hydroxyethylamine derivative **17**^{27,33} in CH₂Cl₂ in the presence of triethylamine at 0 °C to 23 °C for 1 h to furnish hydroxyethylsulfonamide dipeptide isostere **18** with a 4-phenylboronic acid as the P2' ligand in 82% yield.

Synthesis of inhibitors with boronic acid as the P2' ligand is shown in Scheme 3. Boc-derivative **18** was treated with TFA in CH₂Cl₂ at 0 °C for 30 min to provide the corresponding amine. Reaction of the resulting amine with known activated *bis*-THF carbonate derivative **19**²⁹ in the presence of DIPEA in CH₃CN at 23 °C for 10 days furnished inhibitor **5** in 47% yield. Similarly, reaction of resulting amine with activated *crown*-THF carbonate **12** and activated *TP*-THF carbonate **10** afforded inhibitors **6** and **20** in 55% and 51% yields, respectively.

Results and Discussion

Our structure based design strategies resulted in a range of potent PIs with intriguing structural features, particularly PIs with cyclic ether-derived P2 ligands.^{3,14} Through X-ray structural analysis, we have shown that these PIs make extensive interactions particularly with backbone atoms in the active site. In general, these PIs exhibited exceptional enzyme affinity.¹⁴ Even though various factors such as cell penetration and flux, intracellular sequestration may affect antiviral activity, many of these PIs also showed very potent antiviral activity.³ Furthermore, they maintained robust antiviral activity against a wide range of highly multidrug-resistant HIV-1 variants. For the current studies, we designed a selected set of PIs containing carboxylic acid and boronic acid functionalities in the P2'-ligand. These functional groups can form more hydrogen bonds in the S2'-subsite than the aromatic amine functionality of darunavir.⁹ The structure and activity of these PIs are shown in Table 1. We first evaluated these PIs in an enzyme-inhibitory assay.³⁴ As shown, inhibitor **3** with a P2-carboxylic acid showed a K_i value of 12.9 μM . We subsequently determined antiviral activity of these PIs in MT-2 and MT-4 human-T-lymphoid cells exposed to HIV_{LAI}.³⁵ Interestingly, in this cell-based antiviral assay, inhibitor **3** did not exhibit appreciable antiviral activity with IC₅₀ values of 1 μM and 1 mM, in MT-2 and MT-4 cells, respectively. Carboxamide derivative **4** showed very potent enzyme K_i and antiviral IC₅₀ values of 93 nM and 38 nM in MT-2 and MT-4, respectively. Both carboxylic acid containing inhibitors **11** and **13** showed excellent enzyme inhibitory activity (K_i 7.6 and 3.2 μM , respectively) however, they did not show antiviral activity. Boronic acid derivative **5** has been shown to have very potent enzyme inhibitory activity of 0.5 μM .²⁶ However, there is no report of its antiviral activity in a cell-based assay. We have evaluated the boronic acid PI **5** in an antiviral assay with MT-2 cells. It turned out that boronic acid derivative **5** showed improved antiviral IC₅₀ value of 48.9 nM compared to carboxylic derivatives **3** and **4** (entry 2, table 1). We prepared PI **6** containing a crown-like THF ligand as P2 ligand in combination with boronic acid P2' ligand. This inhibitor exhibited an enzyme inhibitory K_i value of 15.5 μM and antiviral activity of 37.7 nM (entry 6). Inhibitor **20** with a (3*aS*,4*S*,7*aR*)-hexahydro-4*H*-furo[2,3-*b*]pyran as the P2 ligand also showed very potent enzyme K_i but much reduced antiviral IC₅₀ value of (120 nM) compared to DRV (entry 7).

Clinically, DRV is used widely for the treatment of naïve and experienced HIV/AIDS patients. However, heavily-ART regimen experienced patients have been showing treatment-failure with approved PIs, including DRV.^{35,36} Therefore, we have examined inhibitors **5** and **6** against DRV-resistant HIV-1 variants and compared their antiviral activity against DRV and one of our preclinical inhibitors, **21**. For these studies, MT-4 cells (1×10^4) are exposed to wild type HIV-1 and three highly DRV-resistant HIV-1 variants, HIV_{DRV}^{R20}, HIV_{DRV}^{Rp30}, and HIV_{DRV}^{Rp51}.^{35,37} These variants were selected by propagating cells with increasing concentrations of DRV and they are highly resistant to all currently approved PIs, including DRV and nucleoside-RT inhibitors, such as tenofovir. Antiviral activity of selected PIs was determined using p24 assays. The results are shown in Table 2. As can be seen, FDA approved PI, LPV was unable to block the replication of these highly DRV-resistant variants. Inhibitor **5**, resulting from incorporation of boronic acid in place of amine in DRV, showed relatively more potent antiviral activity (IC₅₀ value of 219 nM) against DRV-resistant HIV-1

variants selected in the presence of DRV over 20 viral passages (HIV_{DRV}^R_{P20}). Compound **5** lost only 4-fold activity compared to its IC₅₀ values against HIV-1^{WT}. Interestingly, DRV exhibited 164-fold loss of antiviral activity (IC₅₀ 525.8 nM) compared to its IC₅₀ against HIV-1^{WT}. Boronic acid derivative **5** displayed antiviral IC₅₀ of 946 nM (19-fold loss over HIV-1^{WT}) compared to DRV (IC₅₀ 601 nM, 187-fold over HIV-1^{WT}). Both compound **5** and DRV did not exhibit any appreciable antiviral activity against the most highly DRV-resistant HIV-1 variants, HIV_{DRV}^R_{P51}. Inhibitor **6** with a crown-like THF (*Crm*-THF) as the P2-ligand displayed improved antiviral activity compared to inhibitor **5** with a *bis*-THF P2 ligand. It showed antiviral IC₅₀ value of 71 nM against HIV_{DRV}^R_{P20} variants and IC₅₀ value of 532 nM against HIV_{DRV}^R_{P30} variants. Its fold-changes of antiviral activity compared to HIV-1^{WT} are significantly lower than compound **5** or DRV. Compound **6**, however, exhibited antiviral IC₅₀ > 1 μM (>1000-fold change) against highly resistant HIV variants HIV_{DRV}^R_{P51}. One of our recent inhibitors, **21**, showed exceptional antiviral activity against all highly DRV-resistant HIV-1 variants.^{38,39} Both inhibitors **5** and **6** showed no appreciable cytotoxicity in MT-2 cells, with CC₅₀ values of >100 μM, similar to DRV. However, selectivity index (CC₅₀/IC₅₀) were >2,040 and >2,650 compared to 34,480 for DRV and 2,473,684 for compound **21**.

X-ray description

To gain molecular insight into the ligand-binding site interactions of inhibitors **6** (GRL-008–19A) and **20** (GRL-031–19A), we co-crystallized these inhibitors with wild-type HIV-1 protease and the X-ray structures were refined at 1.33 and 1.13 Å resolution with R-factors of 13.7% and 12.5%, respectively. These structures contain a single PR dimer and the inhibitor binds in the active site cavity in two mutually exclusive orientations related by 180° rotation with major/minor occupancies of 60/40% and 65/35% for inhibitors **6** and **20**, respectively. The overall dimer structures are very similar to the HIV-1 protease with DRV (2IEN)¹⁶ with root mean square difference (RMSD) for Cα of 0.20 and 0.12 Å for inhibitors **6** and **20**, respectively. Similarly, the two new structures of inhibitors **6** and **20** are alike (Cα RMSD of 0.14 Å). The urethane NH of both inhibitors forms hydrogen bonding interactions with the carbonyl oxygen of Gly27. In addition, these inhibitors show water-mediated interactions that connect the inhibitor carbonyl oxygen and sulfonamide oxygen with the amides of Ile50 and 50' in the flaps. Similar interactions are shared by the protease-darunavir complex and other protease inhibitors.^{4,16} The key interactions of inhibitor **6** and inhibitor **20** with HIV-1 protease are highlighted in Figure 3.

The hydrogen bond interactions between HIV-1 protease and the two inhibitors were compared with those for DRV. Inhibitors **6** and **20** differ only at the P2-group where the former boasts a *Crm*-THF while the latter contains a tetrahydropyrano-tetrahydrofuran (*Tp*-THF) ligand.^{29,30} Both oxygen atoms of the *Crm*-THF in inhibitor **6** formed a network of hydrogen bonds with the backbone amide NHs of Asp30 and Asp29 in the S2 subsite. These interactions are very similar to what was observed in the X-ray structure of the *Crm*-THF containing inhibitor **21**, described recently.^{38,39} For inhibitor **20**, both oxygens of the *Tp*-THF ligand also formed hydrogen bonds with the backbone amide NHs of Asp30 and Asp29. These interactions are comparable to the equivalent interactions with the *bis*-THF of DRV.^[16,17]

The P2' position of both inhibitors **6** and **20** harbors a phenylboronic acid moiety in place of the 4-aminosulfonamide of DRV. In both crystal structures, the boronic acid is aligned in plane with the phenyl group with less than 2° difference in torsion angle. The boronic acid introduces an additional water-mediated hydrogen bond with the Gly48' amide located on the flexible flap of HIV-1 protease. This interaction is similar to the carboxylic acid derivative **3** as shown in Figure 2. The other hydroxyl group of the boronic acid is within hydrogen bonding distance to both main chain amide of Asp30' (2.7–2.9 Å), although the bond angle departs from the ideal in the crystal structures. It appears that inhibitor **6** makes additional water-mediated interactions in the S2'-site of the active site. Overall, the inhibitor-HIV-1 protease hydrogen bonding interactions resemble those in DRV-HIV-1 protease with the exception of the new water-mediated interaction of boronic acid at P2' and Gly48', which is likely to stabilize the mobile flaps. These new interactions are likely to account for the improved enzyme affinity for inhibitors **6** and **20**. These inhibitors showed better antiviral activity compared to the corresponding carboxylic acid derivatives likely due to improved efflux profiles.

Conclusions

In conclusion, we have designed and synthesized a selected set of HIV-1 protease inhibitors containing benzene carboxylic acid and benzene boronic acid as the P2'-ligands. These ligands are designed to form enhanced hydrogen bonding interactions with the backbone atoms in the S2'-subsite of HIV-1 protease. Inhibitor **3** with P2 *bis*-THF and P2'-benzene carboxylic acid showed potent enzyme inhibitory K_i , but showed no antiviral activity due to poor cell penetration. However, carboxamide derivative **4** displayed excellent enzyme inhibitory activity and good antiviral activity (IC_{50} of 93 nM). The corresponding boronic acid derivative **5** showed excellent enzyme K_i and improvement of antiviral IC_{50} value (49 nM) over the carboxamide derivative. Carboxylic acid and boronic acid containing inhibitors **6** and **13** in combination with a crown-like THF as the P2 ligand also showed very potent enzyme inhibitory activity. Carboxylic acid derivative **13**, however, showed poor antiviral activity. Boronic acid-derived inhibitors displayed potent enzyme activity. They exerted much better antiviral activity in cell-based assay compared to the corresponding carboxylic acid derivatives possibly due to higher efflux profiles. However, DRV with a P2'-aniline ligand displayed significantly more potent antiviral activity compared to boronic acids. We have obtained high resolution X-ray structures of inhibitor **6**-HIV-1 protease and inhibitor **20**-HIV-1 protease complexes. Our structural studies established that both carboxylic acid and boronic acid containing inhibitors are involved in significantly enhanced hydrogen bonding interactions and water-mediated hydrogen bonding interactions in the S2'-site. Inhibitor **5**, while less potent than DRV against HIV_{LAI}^{WT} , exerted comparable antiviral activity against highly DRV-resistant HIV-1 variants, $HIV_{DRV}^{R_{P20}}$ and $HIV_{DRV}^{R_{P30}}$. Inhibitor **6**, with a *Cm*-THF ligand as the P2-ligand, displayed improved antiviral activity compared to *bis*-THF derived inhibitor **5**. Interestingly, fold-change of antiviral activity for boronic acid-derived inhibitors are significantly lower compared to DRV against these highly DRV-resistant HIV-1 variants. Only inhibitor **21** showed potent antiviral activity against $HIV_{DRV}^{R_{P51}}$. Further design of new PIs using the current molecular insight is in progress.

Experimental Section

General—All reactions were carried out under an argon atmosphere in either flame or oven-dried (120 °C) glassware. All reagents and chemicals were purchased from commercial suppliers and used without further purification unless otherwise noted. Anhydrous solvents were obtained as follows: Dichloromethane from calcium hydride, diethyl ether and tetrahydrofuran from Na/Benzophenone, methanol and ethanol from activated magnesium under argon. All purification procedures were carried out with reagent grade solvents (purchased from VWR) in air. TLC analysis was conducted using glass-backed Thin-Layer Silica Gel Chromatography Plates (60 Å, 250 µm thickness, F-254 indicator). Column chromatography was performed using 230–400 mesh, 60 Å pore diameter silica gel. ¹H, ¹³C NMR spectra were recorded at room temperature on a Bruker AV800, DRX-500, ARX-400. Chemical shifts (δ values) are reported in parts per million, and are referenced to the deuterated residual solvent peak. NMR data is reported as: δ value (chemical shift, J-value (Hz), integration, where s = singlet, d = doublet, t = triplet, q = quartet, brs = broad singlet). LRMS and HRMS spectra were recorded at the Purdue University Department of Chemistry Mass Spectrometry Center.

4-(N-((2R,3S)-3-((tert-Butoxycarbonyl)amino)-2-hydroxy-4-phenylbutyl)-N-isobutylsulfamoyl)benzoic acid (9): To a stirred solution of acetal derivative **8** (100 mg, 0.165 mmol) in methanol (6 mL) at 23 °C, potassium carbonate (34 mg, 0.247 mmol) was added. The resulting mixture was stirred at 23 °C for 30 min. The solvent was evaporated under reduced pressure, and the product was extracted with ethyl acetate, dried over anhydrous sodium sulfate and concentrated. The crude product was purified by flash chromatography to provide the corresponding aldehyde (80 mg, 96%).

To a stirred solution of above aldehyde (80 mg, 0.158 mmol) at 23 °C in *t*-BuOH (3.0 mL), were added NaH₂PO₄ (65 mg, 0.476 mmol), 2-methyl-2-butene (170 µL, 1.58 mmol), NaClO₂ (43 mg, 0.476 mmol) and H₂O (1.0 mL). The resulting reaction mixture was allowed stir for 3 h at 23 °C. Then the reaction mixture was extracted with EtOAc and washed with H₂O, brine solution, dried over Na₂SO₄, filtered, and concentrated under reduced pressure to yield crude residue which was purified by column chromatography over silica gel (5% MeOH/CH₂Cl₂) to afford acid inhibitor **9** (75 mg, 90%) as an amorphous solid. ¹H-NMR (400 MHz, Methanol-*d*₄) δ 8.17 (d, *J* = 8.5 Hz, 2H), 7.92 (d, *J* = 8.5 Hz, 2H), 7.27 – 7.18 (m, 4H), 7.15 (m, 1H), 3.71 (ddd, *J* = 9.3, 7.3, 2.5 Hz, 1H), 3.58 (ddd, *J* = 11.0, 7.3, 3.8 Hz, 1H), 3.43 (dd, *J* = 15.1, 2.6 Hz, 1H), 3.18 – 3.02 (m, 3H), 2.95 (dd, *J* = 13.7, 6.8 Hz, 1H), 2.54 (dd, *J* = 13.8, 10.6 Hz, 1H), 2.08 – 1.97 (m, 1H), 1.28 (s, 9H), 0.91 (d, *J* = 6.6 Hz, 3H), 0.87 (d, *J* = 6.6 Hz, 3H); ¹³C-NMR (100 MHz, Methanol-*d*₄) δ 166.7, 156.5, 143.3, 138.7, 134.2, 129.9, 128.9, 127.7, 127.1, 125.6, 78.5, 72.4, 56.7, 55.4, 52.0, 35.8, 27.2, 26.3, 18.9. LRMS-ESI (*m/z*): 521.2 [M+H]⁺.

4-(N-((2R,3S)-3-((((3*a*S,4*S*,7*a*R)-hexahydro-4*H*-furo[2,3-*b*]pyran-4-yl)oxy)carbonyl)amino)-2-hydroxy-4-phenylbutyl)-N-isobutylsulfamoyl)benzoic acid (11): To a stirred solution of **9** (21 mg, 0.04 mmol) in CH₂Cl₂ (1.5 mL) was added TFA (0.5 mL) at 0 °C under argon atmosphere and the mixture was stirred at 23 °C for 3 h. Solvents were evaporated under reduced pressure, then CH₂Cl₂ (3 mL) was added and evaporated

twice to give corresponding amine salt which was used for next step without further purification. The above amine salt (21 mg, 0.04 mmol) was dissolved in acetonitrile (1 mL) and *N,N*-diisopropylethylamine (28 μ L, 0.16 mmol) was added. The resulting mixture was cooled to 0 °C and mixed carbonate **10** (10 mg, 0.03 mmol) was added to it. The resulting reaction mixture was allowed to warm to 23 °C and stir under argon for 12 d. After this period, the reaction mixture was diluted with a mixture of 10% MeOH in CH₂Cl₂ (10 mL), transferred to a separatory funnel, and washed with 1M HCl (2 mL). The organic layer was dried over Na₂SO₄, filtered, and concentrated under reduced pressure to afford a crude solid which was purified by silica gel chromatography (5% MeOH/CH₂Cl₂) to yield the desired inhibitor **11** as an amorphous white solid (7.1 mg, 37%). *R*_f = 0.70 (silica plate, 20% MeOH/CH₂Cl₂). ¹H-NMR (800 MHz, CD₃OD) δ 8.17 (d, *J* = 8.1 Hz, 2H), 7.92 (d, *J* = 8.2 Hz, 2H), 7.30 – 7.14 (m, 5H), 6.97 (d, *J* = 8.6 Hz, 1H), 4.91 (s, 1H), 4.06 (t, *J* = 9.1 Hz, 1H), 3.96 – 3.68 (m, 4H), 3.44 (d, *J* = 15.1 Hz, 1H), 3.38 (t, *J* = 12.3 Hz, 1H), 3.16 (d, *J* = 14.0 Hz, 2H), 3.04 (dd, *J* = 15.4, 8.1 Hz, 1H), 2.97 – 2.91 (m, 1H), 2.53 (t, *J* = 12.2 Hz, 1H), 2.31 (s, 1H), 2.03 (s, 1H), 1.85 (p, *J* = 11.3, 10.5 Hz, 1H), 1.72 (q, *J* = 12.5 Hz, 1H), 1.65 (d, *J* = 13.4 Hz, 1H), 1.42 (d, *J* = 10.1 Hz, 1H), 1.37 (s, 1H), 0.93 (d, *J* = 5.6 Hz, 3H), 0.89 (d, *J* = 6.0 Hz, 3H). ¹³C-NMR (200 MHz, CD₃OD) δ 157.8, 144.4, 140.3, 131.4, 130.5, 129.2, 128.6, 127.1, 102.4, 74.1, 71.0, 69.3, 61.8, 58.4, 57.3, 53.6, 44.8, 37.3, 27.9, 27.4, 23.2, 20.3. HRMS (ESI) *m/z*: [M + Na]⁺ Calcd for C₂₉H₃₈N₂O₉S 613.2190; Found 613.2174.

4-(N-((2*R*,3*S*)-3-(((3*S*,7*aS*,8*S*)-Hexahydro-4*H*-3,5-methanofuro[2,3-*b*]pyran-8-yl)oxy)carbonyl)amino)-2-hydroxy-4-phenylbutyl)-N-isobutylsulfamoyl)benzoic acid (13**):**

To a stirred solution of **9** (25 mg, 0.048 mmol) in CH₂Cl₂ (1.5 mL) was added TFA (0.5 mL) at 0 °C under argon atmosphere and the mixture was stirred at 23 °C for 3 h. Solvents were evaporated under reduced pressure, then CH₂Cl₂ (3 mL) was added and evaporated twice to give corresponding amine which was used for next step without further purification. The above amine was dissolved in acetonitrile (1 mL) and then added DIPEA (33 μ L, 0.187 mmol) at 0 °C under argon atmosphere. To this reaction mixture, activated *crown*-THF carbonate **12** (12 mg, 0.037 mmol) was added and stirred at 23 °C for 7 days. Volatiles were evaporated under reduced pressure and the crude residue was purified by column chromatography over silica gel to provide inhibitor **13** (23 mg) as an amorphous solid (80 % yield over two steps). ¹H NMR (400 MHz, Methanol-*d*₄) δ 8.16 (d, *J* = 8.5 Hz, 2H), 7.91 (d, *J* = 8.5 Hz, 2H), 7.28 – 7.20 (m, 5H), 7.16 (m, 1H), 5.33 (d, *J* = 6.2 Hz, 1H), 4.69 (dd, *J* = 9.1, 5.6 Hz, 1H), 3.95 (d, *J* = 11.3 Hz, 1H), 3.78 – 3.67 (m, 2H), 3.62 – 3.53 (m, 2H), 3.43 (dd, *J* = 15.1, 2.5 Hz, 1H), 3.38 (dd, *J* = 9.3, 5.9 Hz, 1H), 3.16 (ddd, *J* = 13.7, 5.6, 2.4 Hz, 2H), 3.03 (dd, *J* = 15.0, 8.4 Hz, 1H), 2.94 (dd, *J* = 13.6, 6.8 Hz, 1H), 2.68 – 2.60 (m, 2H), 2.54 (dd, *J* = 13.9, 10.8 Hz, 1H), 2.32 (q, *J* = 6.3 Hz, 1H), 2.02 (ddd, *J* = 12.7, 7.9, 6.3 Hz, 1H), 1.76 (d, *J* = 12.0 Hz, 1H), 1.49 (dt, *J* = 12.2, 3.9 Hz, 1H), 1.36 (m, 1H), 0.92 (d, *J* = 6.5 Hz, 3H), 0.87 (d, *J* = 6.6 Hz, 3H); ¹³C NMR (125 MHz, Methanol-*d*₄) δ 166.7, 156.3, 143.0, 138.7, 134.3, 129.9, 128.9, 127.8, 127.1, 125.7, 104.2, 74.6, 72.6, 67.9, 59.5, 56.8, 56.0, 52.0, 44.6, 41.9, 37.3, 35.7, 26.4, 22.7, 18.9. LRMS-ESI (*m/z*): 603.2 [M+H]⁺. HRMS-ESI (*m/z*): [M+H]⁺ calcd for C₃₀H₃₉N₂O₉S, 603.2371; found 603.2360.

(4-(methoxysulfonyl)phenyl)boronic acid (15**):** To a stirred solution of 4-bromophenylsulfonyl chloride (2.55 g, 10 mmol) in methanol (20 mL) was added NaOMe

(810 mg, 15 mmol) at 0 °C. The reaction was stirred at 23 °C for 12 h and TLC showed the complete consumption of the starting material. The solvent was removed under vacuum and water was added to the residue. The mixture was extracted with a mixture (15:1) of CH₂Cl₂ and methanol. The combined organic layer was washed with brine, dried over Na₂SO₄ and filtered. The solvent was removed under reduced pressure and the residue was purified by silica gel column chromatography (ethyl acetate/hexane 1:20 to 1:15) to afford the corresponding methyl ester (1.56 g, 62% yield). ¹H-NMR (400 MHz, CD₃OD) δ 7.81 (s, 4H), 3.76 (s, 3H). ¹³C-NMR (100 MHz, CD₃OD) δ 134.3, 132.4, 129.3, 128.5, 56.1. MS (ESI) calcd for C₇H₈BrO₃S [M+H]⁺: 250.9, Found: 250.9, 252.9.

To a stirred solution of above ester (2.50 g, 10 mmol) in THF (20 mL) under argon at -78 °C, n-BuLi (1.6 M in hexane, 6.9 mL, 11 mmol) was added. The reaction was stirred at -78 °C for 10 min and B(OMe)₃ (1.68 mL, 15 mmol) was added. The reaction was continued to stir at -78 °C for additional 30 min. The reaction was quenched with aqueous NH₄Cl solution. The mixture was extracted with ethyl acetate/hexane (ethyl acetate/hexane 1:3) and the organic layer was discarded. The aqueous layer was adjusted to pH 6 and the mixture was extracted with a mixture (15:1) of CH₂Cl₂ and methanol. The combined organic layer was washed with brine, dried over Na₂SO₄ and filtrated. The solvent was removed under reduced pressure to obtain the crude boronic acid derivative **15** (970 mg, 45% yield). This was used for the next step without purification. ¹H-NMR (400 MHz, CD₃OD) δ 7.91 (br s, 2H), 7.84 (d, *J* = 8.0 Hz, 2H), 3.72 (s, 3H). ¹³C-NMR (100 MHz, CD₃OD) δ 136.1, 134.1, 126.4, 55.8. MS (ESI) calcd for C₇H₁₁BO₆S [M+H₂O]⁺: 234.0, Found: 234.0; calcd for C₇H₉BNaO₅S [M+Na]⁺: 239.0, Found: 239.0; calcd for C₇H₁₀BO₅S [M+H]⁺: 217.0, Found: 217.0.

(4-(chlorosulfonyl)phenyl)boronic acid (16): To a stirred solution of boronic acid derivative **15** (1.08 g, 5 mmol) in methanol (10 mL) at 23 °C, was added TEA (2.8 mL, 20 mmol). The resulting reaction mixture was heated to 60 °C for 24 h. After this period, the solvent was removed completely under vacuum and the residue was used for the next step without purification.

To a stirred solution of the above residue at 0 °C, SOCl₂ (10 mL) was added. The reaction mixture was warmed to 23 °C and then heated to 80 °C for 24 h. After this period, the reaction mixture was concentrated under reduced pressure and the resulting residue was carefully quenched with crushed ice. The mixture was extracted with CH₂Cl₂. The combined organic layer was washed with brine, dried over Na₂SO₄ and filtrated. The solvent was removed under reduced pressure to give the title sulfonyl chloride **16** (980 mg slightly yellow solid, 89% yield over two steps). This sulfonyl chloride is sufficiently pure and was used for the next step without purification. An analytical sample was prepared by recrystallization in hexane. MP: decomposed at 110 °C. ¹H-NMR (400 MHz, CD₃OD) δ 8.06–8.01 (m, 2H), 7.91–7.97 (m, 2H). ¹³C-NMR (100 MHz, CD₃OD) δ 144.9, 134.5, 125.3. MS (EI) calcd for C₆H₆ClO₂S [M-B(OH)₂+2H]⁺: 177.0, Found: 177.0, 179.0.

(4-(N-((2R,3S)-3-((tert-butoxycarbonyl)amino)-2-hydroxy-4-phenylbutyl)-N-isobutylsulfamoyl)phenyl)boronic acid (18): To a stirred solution of amine **17** (336 mg, 1 mmol) in CH₂Cl₂ (10 mL) at 0 °C, sulfonyl chloride **16** (264 mg, 1.2 mmol) followed by

Et₃N (0.7 mL, 5 mmol) were added. The resulting reaction mixture was stirred at 23 °C for 1 h and TLC showed the complete consumption of the secondary amine. The reaction was quenched with ice water and adjust to pH 6 with 1 N HCl. The mixture was extracted with a mixture (15:1) of CH₂Cl₂ and methanol. The combined organic layer was washed with brine, dried over Na₂SO₄, and filtrated. After the solvent was removed under reduced pressure, the residue was purified by silica gel column chromatography (CH₂Cl₂ and methanol 50:1 to 15:1) to afford sulfonamide **18** (425 mg, 82% yield). ¹H-NMR (400 MHz, CD₃OD, two rotamers) δ 7.95–7.70 (m, 4H), 7.25–7.09 (m, 5H), 3.80–3.57 (m, 2H), 3.46–3.56 (m, 1H), 3.15–2.83 (m, 4H), 2.60–2.44 (m, 1H), 2.05–1.93 (m, 1H), 1.27, 1.15 (s, 9H), 0.88 (d, 6.4 Hz, 3H), 0.84 (d, 6.4 Hz, 3H). ¹³C-NMR (100 MHz, CD₃OD, major rotamer) δ 156.4, 140.2, 138.7, 133.9, 129.3, 129.0, 127.7, 126.0, 125.9, 125.6, 78.6, 72.7, 57.2, 55.3, 52.4, 35.8, 27.3, 26.5, 19.1. MS (ESI) calcd for C₂₁H₃₀BN₂O₇S [M-C₄H₇]⁺: 465.2, Found: 465.1; calcd for C₂₅H₃₈BN₂O₇S [M+H]⁺: 521.3, Found: 521.3.

(4-(N-((2R,3S)-3-(((3R,3aS,6aR)-hexahydrofuro[2,3-b]furan-3-yl)oxy)carbonyl)amino)-2-hydroxy-4-phenylbutyl)-N-isobutylsulfamoyl)phenyl)boronic acid (5): To a stirred solution of Boc-derivative **18** (21 mg, 0.04 mmol) in CH₂Cl₂ (1.5 mL) at 0 °C, TFA (0.5 mL) was added. The resulting reaction mixture was stirred at 0 °C for 30 min. The reaction mixture was concentrated under reduced pressure and ice water (2 mL) was added to the residue. The pH was adjusted to neutral with 2.5 N NaOH. The mixture was extracted with a mixture (15:1) of CH₂Cl₂ and methanol. The combined organic layer was washed with brine, dried over Na₂SO₄ and filtrated. The solvent was removed under reduced pressure, the resulting crude amine was used for the next step without purification.

To a stirred solution of the above amine in CH₃CN (1.0 mL), DIPEA (70 μL, 10 equiv) followed by mixed carbonate **19** (13 mg, 0.04 mmol) were added. The resulting reaction mixture was stirred at 23 °C for 10 days. After this period, the solvent was removed under reduced pressure and 1 N HCl was added to the residue and the pH was adjusted to about 6. The mixture was extracted with a mixture (15:1) of CH₂Cl₂ and methanol. The combined organic layer was washed with brine, dried over Na₂SO₄ and filtrated. The solvent was removed under reduced pressure and the residue was purified by silica gel column chromatography (CH₂Cl₂: methanol:HCO₂H, 100:2:1 to 100:5:1) to afford inhibitor **5** (11 mg, 47% yield) as an amorphous solid. The proton spectrum is identical with the reported one.³ Analytical data: ¹H-NMR (400 MHz, CD₃OD) δ 7.87–7.77 (m, 4H), 7.26–7.16 (m, 5H), 5.59 (d, *J* = 5.2 Hz, 1H), 4.97–4.91 (m, 1H), 3.94 (dd, *J* = 9.6, 6.0 Hz, 1H), 3.83–3.64 (m, 5H), 3.45 (dd, *J* = 14.8, 2.4 Hz, 1H), 3.23–3.10 (m, 2H), 3.01–2.84 (m, 3H), 2.53 (dd, *J* = 14.0, 10.8 Hz, 1H), 2.09–1.99 (m, 1H), 1.56–1.47 (m, 1H), 1.38–1.32 (m, 1H), 0.94 (d, *J* = 6.4 Hz, 3H), 0.88 (d, *J* = 6.4 Hz, 3H). ¹³C-NMR (200 MHz, CD₃OD) δ 157.8, 157.7, 140.3, 135.1, 130.5, 129.3, 127.4, 127.2, 110.8, 74.6, 74.5, 72.1, 70.6, 58.9, 57.4, 53.9, 46.9, 37.1, 28.0, 27.0, 20.5, 20.4. MS (ESI) calcd for C₂₇H₃₈BN₂O₉S [M+H]⁺: 577.2, Found: 577.3.

(4-(N-((2R,3S)-3-(((3S,7aS,8S)-Hexahydro-4H-3,5-methanofuro[2,3-b]pyran-8-yl)oxy)carbonyl)amino)-2-hydroxy-4-phenylbutyl)-N-isobutylsulfamoyl)phenyl)boronic acid (6): Following the procedure outlined for inhibitor **5**, reaction of amine derived from Boc-derivative **18** (20 mg, 0.04 mmol) and activated *crown*-THF carbonate **12** (10 mg, 0.031

mmol) afforded inhibitor **6** (12.5 mg, 55% for 2-steps) as an amorphous solid. $^1\text{H-NMR}$ (400 MHz, Methanol- d_4) δ 7.79 (s, 5H), 7.30 – 7.21 (m, 4H), 7.19 – 7.13 (m, 1H), 5.34 (d, J = 6.2 Hz, 1H), 4.71 – 4.64 (m, 1H), 3.95 (d, J = 11.2 Hz, 1H), 3.81 – 3.67 (m, 2H), 3.61 – 3.54 (m, 2H), 3.47 – 3.35 (m, 2H), 3.26 – 3.20 (m, 1H), 3.17 (dd, J = 14.0, 3.4 Hz, 1H), 3.10 (dd, J = 13.6, 8.1 Hz, 1H), 3.02 – 2.80 (m, 2H), 2.73 – 2.60 (m, 2H), 2.55 (dd, J = 13.8, 11.0 Hz, 1H), 2.32 (m, 1H), 2.06 – 1.96 (m, 1H), 1.76 (d, J = 12.0 Hz, 1H), 1.48 (dt, J = 12.1, 3.9 Hz, 1H), 0.91 (d, J = 6.6 Hz, 3H), 0.86 (d, J = 6.9 Hz, 3H); $^{13}\text{C-NMR}$ (200 MHz, Methanol- d_4) δ 156.4, 138.8, 133.7, 129.1, 128.8, 127.9, 126.0, 125.8, 104.3, 74.7, 73.0, 72.1, 68.0, 59.7, 57.4, 56.1, 56.0, 55.0, 53.4, 52.5, 48.1, 44.7, 42.0, 37.4, 35.8, 26.6, 22.8, 19.1, 19.0. LRMS-ESI (m/z): 603.2 $[\text{M}+\text{H}]^+$. HRMS-ESI (m/z): $[\text{M}+\text{Na}]^+$ calcd for $\text{C}_{29}\text{H}_{39}\text{BN}_2\text{O}_9\text{SNa}$, 624.2398; found 624.2393.

(4-(N-((2R,3S)-3-((((3aS,4S,7aR)-hexahydro-4H-furo[2,3-b]pyran-4-yl)oxy)carbonyl)amino)-2-hydroxy-4-phenylbutyl)-N-isobutylsulfamoyl)phenyl)boronic acid (20): Following the procedure outlined for inhibitor **5**, reaction of amine salt derived from Boc-derivative **18** (21 mg, 0.04 mmol) and activated carbonate **10** (13.6 mg, 0.04 mmol) afforded inhibitor **20** (12 mg, 51%) as an amorphous solid. $^1\text{H-NMR}$ (400 MHz, CD_3OD , two isomers) δ 7.79 (br s, 4H), 7.31–7.09 (m, 5H), 4.92–4.86 (m, 2H), 4.05 (t, J = 7.6 Hz, 1H), 3.84–3.70 (m, 4H), 3.46–3.32 (m, 2H), 3.21–3.06 (m, 2H), 3.02–2.84 (m, 2H), 2.57–2.49 (m, 1H), 2.35–2.25 (m, 1H), 2.07–1.95 (m, 1H), 1.92–1.79 (m, 1H), 1.78–1.60 (m, 2H), 1.46–1.36 (m, 1H), 0.91 (d, 6.4 Hz, 3H), 0.86 (d, 6.4 Hz, 3H). $^{13}\text{C-NMR}$ (100 MHz, CD_3OD , major isomer) δ 156.2, 139.7, 138.8, 133.6, 129.2, 129.0, 127.7, 125.9, 125.6, 100.9, 72.8, 69.4, 67.8, 60.2, 57.3, 55.7, 55.6, 52.4, 43.3, 35.7, 26.5, 25.8, 21.7, 18.9. HRMS (ESI) calcd for $\text{C}_{28}\text{H}_{39}\text{BN}_2\text{O}_9\text{SNa}$ $[\text{M}+\text{Na}]^+$: 612.2398, Found: 612.2391.

Determination of X-ray structures of HIV-1 protease-inhibitor complexes for inhibitors **6** and **20**:

HIV-1 PR optimized for bacterial expression was purified as described.⁴⁰ PR at 4.2 mg/mL was complexed with inhibitor at 5:1 molar ratio. Crystals of protease-inhibitor complexes were grown by hanging drop vapor diffusion with well solutions of 1.4 M sodium chloride, 0.1 M sodium acetate buffer pH 6.0 and 1.3 M sodium chloride, 0.1 M sodium acetate pH 6.2 reservoir solution for inhibitors **6** and **20**, respectively. Streak-seeding was employed to induce crystallization for inhibitor **6**. Crystals were cryo-cooled to 90 K and 1.0 Å wavelength X-ray diffraction data was collected on beamline 22-ID at SER-CAT, Advanced Photon Source, Argonne National Lab (Chicago, IL, USA). Data were processed and scaled using HKL2000.⁴¹ The structures were solved by molecular replacement in PHASER⁴² in CCP4i suite,^{43,44} using PR-APV (PDB: 3NU3)⁴⁵ as an isomorphous model and refined with COOT,^{46,47} and Refmac5 in CCP4i, using anisotropic displacement parameters (B-factors).⁴⁸ JLignad⁴⁹ in CCP4i, was used to generate refinement restraints for inhibitors. Crystallographic statistics are supplied in Table 1. Coordinates and structure factors for inhibitors **6** (GRL-008–19A) and **20** (GRL-031–19A) were deposited in the Protein Data Bank,⁵⁰ with accession codes codes 6U7O and 6U7P.

Supplementary Material

Refer to Web version on PubMed Central for supplementary material.

Acknowledgements

The present research was supported by grants from the National Institutes of Health AI150466 (AKG) and AI150461 (ITW). DWK is supported by Georgia State University Molecular Basis of Disease Fellowship. This work was also supported in part by the Intramural Research Program of the Center for Cancer Research, National Cancer Institute, National Institutes of Health (HM: R01AI121315); a Grant-in-Aid for Scientific Research (Priority Areas) from the Ministry of Education, Culture, Sports, Science, and Technology of Japan (Monbu-Kagakusho), a Grant for Promotion of AIDS Research from the Ministry of Health, Welfare, and Labor of Japan; grants from Japan Agency for Medical Research and Development (AMED)(HM: JP15fk0410001 and JP18fk0410001); and grants from National Center for Global Health and Medicine Research Institute (HM). We thank the staff at the Southeast Regional-Collaborative Access Team (SER-CAT) at the Advanced Photon Source, Argonne National Laboratory, for assistance during X-ray data collection. Use of the Advanced Photon Source was supported by the U. S. Department of Energy, Office of Science, Office of Basic Energy Sciences, under Contract No. W-31-109-Eng-38. We also thank the Purdue University Center for Cancer Research, which supports the shared NMR and mass spectrometry facilities.

References:

- [1]. Ghosh AK, Gemma S. Structure-based Design of Drugs and Other Bioactive Molecules: Tools and Strategies; Wiley-VCH; 2014: 337–354.
- [2]. Hubbard RE, Structure-based Drug Discovery: An Overview RSC Publishing, 2006.
- [3]. Ghosh AK, Osswald HL, Prato G, J. Med. Chem 2016, 59, 5172–5208. [PubMed: 26799988]
- [4]. Wlodawer A, Vondrasek J, Annu. Rev. Biophys. Biomol. Struct 1998, 27, 249–284. [PubMed: 9646869]
- [5]. Broder S, Antiviral Res. 2010, 85, 1–18. [PubMed: 20018391]
- [6]. Edmonds A, Yotebieng M, Lusiana J, Matumona Y, Kitetele F, Napravnik S, Cole SR, Van Rie A, Behets F, PLoS Med. 2011, 8, e1001044. [PubMed: 21695087]
- [7]. Peng C, Ho BK, Chang TW, Chang NT. J. Virol 1989, 63, 2550–2556. [PubMed: 2657099]
- [8]. Kohl NE, Emini EA, Schleif WA, Davis LJ, Heimbach JC, Dixon RA, Scolnick EM, Sigal IS. Proc. Natl. Acad. Sci. USA 1988, 85, 4686–4696. [PubMed: 3290901]
- [9]. Ghosh AK, Dawson ZL, Mitsuya H, Bioorg. Med. Chem 2007, 15, 7576–7580. [PubMed: 17900913]
- [10]. de Bethune MP, Sekar V, Spinosa-Guzman S, Vanstockem M, De Meyer S, Wigerinck P, Lefebvre E, Darunavir (Prezista, TMC114): from Bench to Clinic, Improving Treatment Options for HIV-infected Patients in Antiviral Drugs: from Basic Discovery through Clinical Trials, John Wiley & Sons, Inc., New Jersey, 2011, pp. 31e45.
- [11]. Guidelines for the use of antiretroviral agents in HIV-1-infected adults and adolescents <https://aidsinfo.nih.gov/contentfiles/lvguidelines/adultandadolescentgl.pdf>, accessed on March 31, 2018.
- [12]. Hué S, Gifford RJ, Dunn D, Fernhill E, Pillay D, J. Virol 2009, 83, 2645–2654. [PubMed: 19158238]
- [13]. Hayashi H, Takamune N, Nirasawa T, Aoki M, Morishita Y, Das D, Koh Y, Ghosh AK, Misumi S, Mitsuya H, Proc. Natl. Acad. Sci 2014, 111, 12234–12239. [PubMed: 25092296]
- [14]. Ghosh AK, Anderson DD, Weber IT, Mitsuya H, Angew. Chem. Int. Ed 2012, 51, 1778–1802.
- [15]. Ghosh AK, Chapsal B, Weber IT, Mitsuya H, Acc. Chem. Res 2008, 41, 78–86. [PubMed: 17722874]
- [16]. Tie Y, Boross PI, Wang Y-F, Gaddis L, Hussian AK, Leshchenko S, Ghosh AK, Louis JM, Harrison RW, Weber IT, J. Mol. Biol 2004, 338, 341–352. [PubMed: 15066436]
- [17]. Kovalevsky AY, Liu F, Leshchenko S, Ghosh AK, Louis JM, Harrison RW, Weber IT, J. Mol. Biol 2006, 363, 161–173. [PubMed: 16962136]

- [18]. Koh Y, Nakata H, Maeda K, Ogata H, Bilcer G, Devasamudram T, Kincaid JF, Boross P, Wang Y-F, Tie Y, Volarath P, Gaddis L, Harrison RW, Weber IT, Ghosh AK, Mitsuya H, *Antimicrob. Agents Chemother* 2003, 47, 3123–3129. [PubMed: 14506019]
- [19]. De Meyer S, Azijn H, Surleraux D, Jochmans D, Tahri A, Pauwels R, Wigerinck P, de Bethune MP, *Antimicrob. Agents Chemother* 2005, 49, 2314–2321. [PubMed: 15917527]
- [20]. Sterrantino G, Zaccarelli M, Colao G, Baldanti F, Di Giambenedetto S, Carli T, Maggiolo F, Zazzi M, *Infection* 2012, 40, 311–318. [PubMed: 22237471]
- [21]. De Meyer S, Lathouwers E, Dierynck I, De Paepe E, Van Baelen B, Vangeneugden T, Spinosa-Guzman S, Lefebvre E, Picchio G, de Béthune M-P, *AIDS*, 2009, 23, 1829–1840. [PubMed: 19474650]
- [22]. Yedidi RS, Maeda K, Fyvie WS, Steffey M, Davis DA, Palmer I, Aoki M, Kaufman JD, Stahl SJ, Garimella H, Das D, Wingfield PT, Ghosh AK, Mitsuya H, *Antimicrob. Agents and Chemother* 2013, 57, 4920–4927. [PubMed: 23877703]
- [23]. Zhou S-F, *Xenobiotica* 2008, 38, 802–832. [PubMed: 18668431]
- [24]. Hoggard PG, Owen A, *Antimicrob. Chemother* 2003, 51, 493–496.
- [25]. Fujimoto H, Higuchi M, Watanabe H, Koh Y, Ghosh AK, Mitsuya H, Tanoue N, Hamada A, Saito H. *Biol. Pharm. Bull* 2009, 32, 1588–1593. [PubMed: 19721237]
- [26]. Windsor IW, Palte MJ, Lukesh III JC, Gold B, Forest KT, Raines RT, *J. Am. Chem. Soc* 2018, 140, 14015–14018. [PubMed: 30346745]
- [27]. Ghosh AK, Sridhar PR, Leshchenko S, Hussain AK, Li J, Kovalevsky AY, Walters DE, Wedekind J, Grum-Tokars V, Das D, Koh Y, Maeda K, Gatanaga H, Weber IT, Mitsuya H, *J. Med. Chem* 2006, 49, 5252–5261. [PubMed: 16913714]
- [28]. Bal BS, Childers WE, Pinnick HW, *Tetrahedron* 1981, 37, 2091–2096.
- [29]. Ghosh AK, Chapsal BD, Parham GL, Steffey M, Agniswamy J, Wang Y-F, Amano M, Weber IT, Mitsuya H *J. Med. Chem* 2011, 54, 5890–5901. [PubMed: 21800876]
- [30]. Ghosh AK, Rao KV, Nyalapatla PR, Osswald HL, Martyr CD, Aoki M, Hayashi H, Agniswamy J, Wang YF, Bulut H, Das D, Weber IT, Mitsuya H, *J. Med. Chem* 2017, 60, 4267–4278. [PubMed: 28418652]
- [31]. Kunst E, Gallier F, Dujardin G, Yusubov MS, Kirschning A *Org. Lett* 2007, 9, 5199–5202. [PubMed: 17999512]
- [32]. Sulfonyl chloride 16 is quite stable. The preliminary X-ray structure shows mixed conformational isomers. Further refinement is in progress.
- [33]. Ghosh AK, Fyvie WS, Brindisi M, Steffey M, Agniswamy J, Wang Y-F, Aoki M, Amano M, Weber IT, Mitsuya H. *ChemMedChem* 2017, 12, 1942–1952. [PubMed: 29110408]
- [34]. Toth MV, Marshall GR, *Int. J. Pept. Protein Res* 1990, 36, 544–550. [PubMed: 2090647]
- [35]. Koh Y, Amano M, Towata T, Danish M, Leshchenko-Yashchuk S, Das D, Nakayama M, Tojo Y, Ghosh AK, Mitsuya H, *J. Virol* 2010, 84, 11961–11969. [PubMed: 20810732]
- [36]. De Meyer S, Lathouwers E, Dierynck I, De Paepe E, Van Baelen B, Vangeneugden T, Spinosa-Guzman S, Lefebvre E, Picchio G, de Béthune MP, *AIDS* 2009, 23, 1829–1840. [PubMed: 19474650]
- [37]. Smart BE, *J. Fluor. Chem* 2001, 109, 3–11.
- [38]. Aoki M, Hayashi H, Rao KV, Das D, Higashi-Kuwata N, Bulut H, Aoki-Ogata H, Takamatsu Y, Yedidi RS, Davis DA, Hattori S.-i., Nishida N, Hasegawa K, Takamune N, Nyalapatla PR, Osswald HL, Jono H, Saito H, Yarchoan R, Misumi S, Ghosh AK, Mitsuya H, *eLife* 2017, 6, e28020. [PubMed: 29039736]
- [39]. Ghosh AK, Rao KV, Nyalapatla PR, Kovala S, Brindisi M, Osswald HL, Sekhara Reddy B, Agniswamy J, Wang YF, Aoki M, Hattori SI, Weber IT and Mitsuya H, *ChemMedChem* 2018, 13, 803–815. [PubMed: 29437300]
- [40]. Sayer JM, Agniswamy J, Weber IT, Louis JM *Protein Sci.* 2010, 19, 2055–2072. [PubMed: 20737578]
- [41]. Otwinowski Z, Minor W, *Processing of X-ray Diffraction Data Collected in Oscillation Mode. Methods in Enzymology, 276: Macromolecular Crystallography, Part A*; Carter CW Jr., Sweet RM, Eds.; Academic Press: New York, 1997; pp 307–326.

- [42]. McCoy AJ, Grosse-Kunstleve RW, Adams PD, Winn MD, Storoni LC, Read RJ, *J. Appl. Crystallogr* 2007, 40, 658–674. [PubMed: 19461840]
- [43]. Winn MD, Ballard CC, Cowtan KD, Dodson EJ, Emsley P, Evans PR, Keegan RM, Krissinel EB, Leslie AGW, McCoy A, McNicholas SJ, Murshudov GN, Pannu NS, Potterton EA, Powell HR, Read RJ, Vagin A, Wilson KS, *Acta Crystallogr., Sect. D: Biol. Crystallogr* 2011, 67, 235–242. [PubMed: 21460441]
- [44]. Potterton E, Briggs P, Turkenburg M, Dodson E, *Acta Crystallogr., Sect. D: Biol. Crystallogr* 2003, 59, 1131–1137. [PubMed: 12832755]
- [45]. Shen C-H, Wang Y-F, Kovalevsky AY, Harrison RW, Weber IT, *FEBS J.* 2010, 277, 3699–3714. [PubMed: 20695887]
- [46]. Emsley P, Lohkamp B, Scott WG, Cowtan K, *Acta Crystallogr., Sect. D: Biol. Crystallogr* 2010, 66, 486–501. [PubMed: 20383002]
- [47]. Emsley P, Cowtan K, *Acta Crystallogr., Sect. D: Biol. Crystallogr* 2004, 60, 2126–2132. [PubMed: 15572765]
- [48]. Murshudov GN, Vagin AA, Dodson EJ, *Acta Crystallogr. D Biol. Crystallogr* 1997, 53, 240–255.
- [49]. Lebedev AA, Young P, Isupov MN, Moroz OV, Vagin AA, Murshudov GN, *Acta Crystallogr. D. Biol. Crystallogr* 2012, 68, 431–440.
- [50]. Berman HM, Westbrook J, Feng Z, Gilliland G, Bhat TN, Weissig H, Shindyalov IN, Bourne PE, *Nucleic Acids Res.* 2000, 28, 235–242. [PubMed: 10592235]

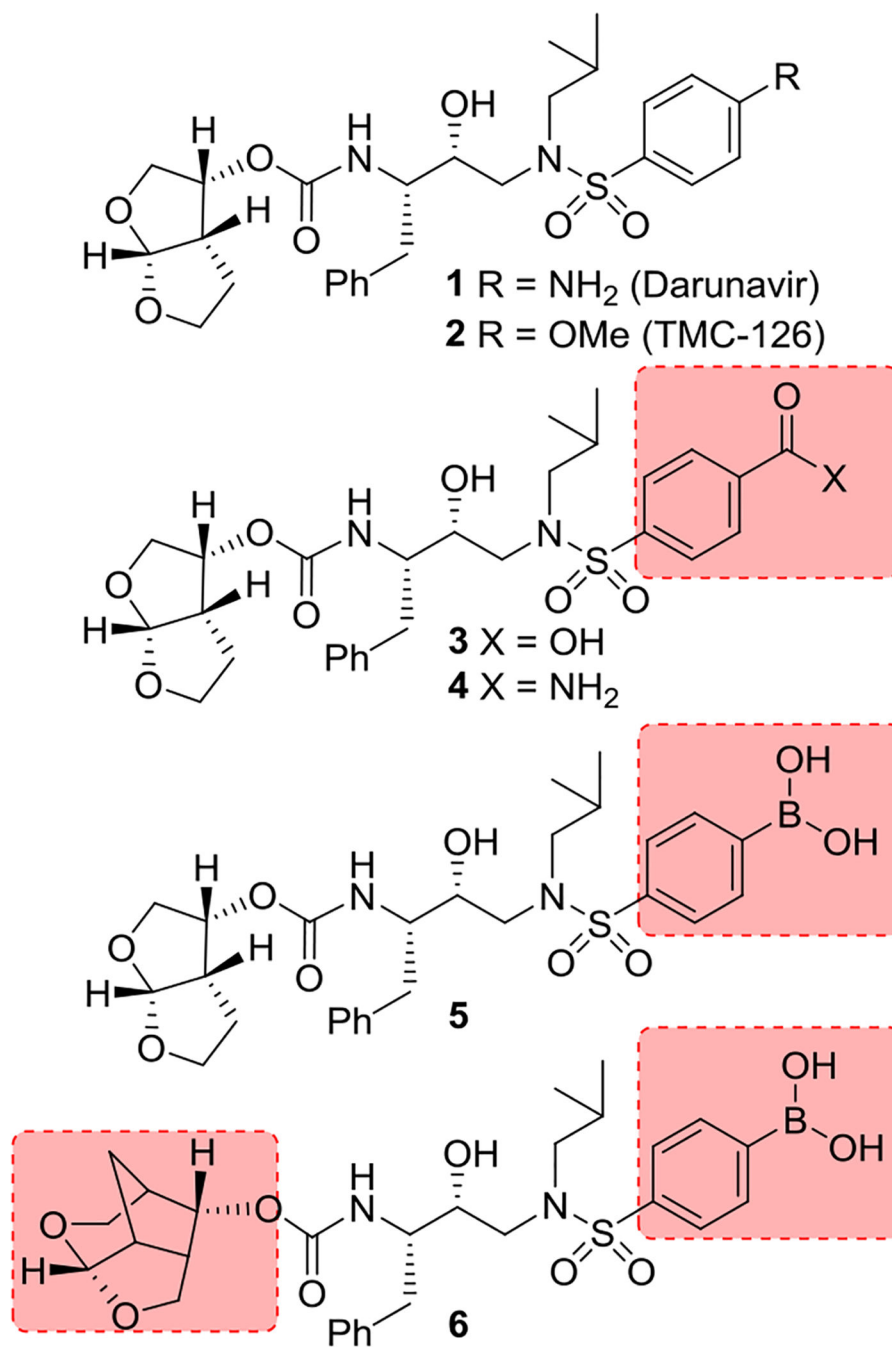


Figure 1.
Structures of HIV-1 protease inhibitors **1-6**.

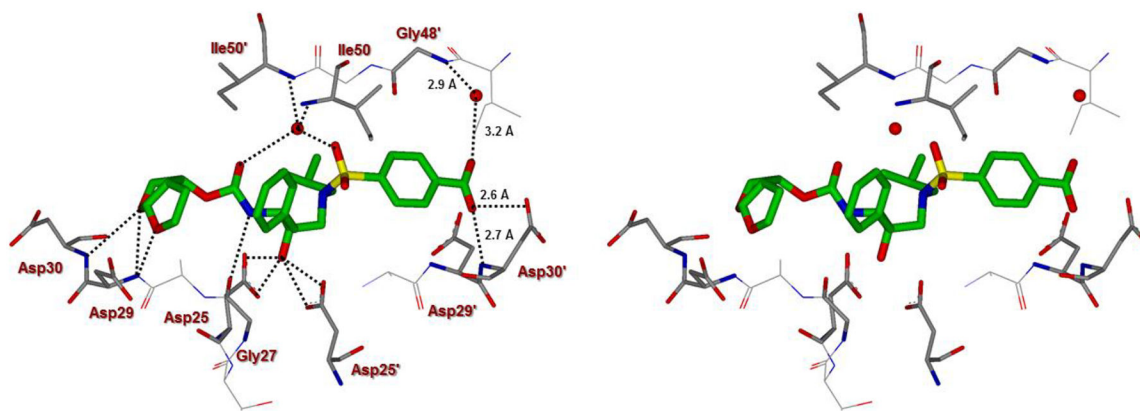


Figure 2.

A stereoview of inhibitor **3**-bound X-ray structure of HIV-1 protease. The major orientation of the inhibitor is shown. The inhibitor carbon atoms are shown in green, water molecules are red spheres, and the hydrogen bonds are indicated by dotted lines (PDB ID: 4I8W).

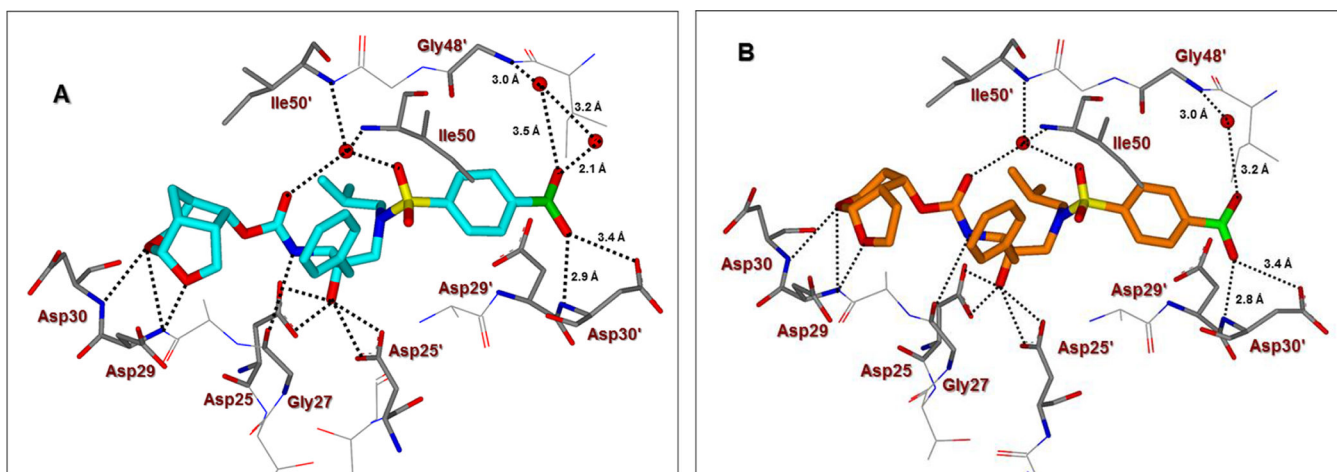
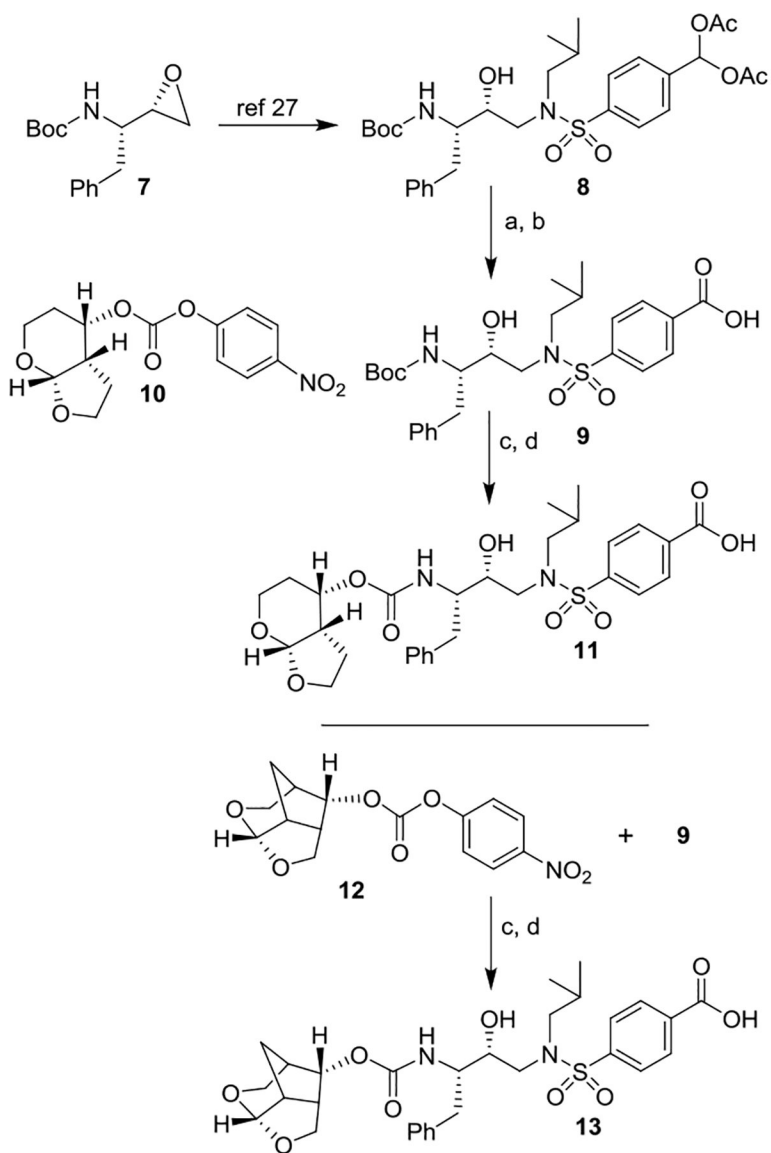
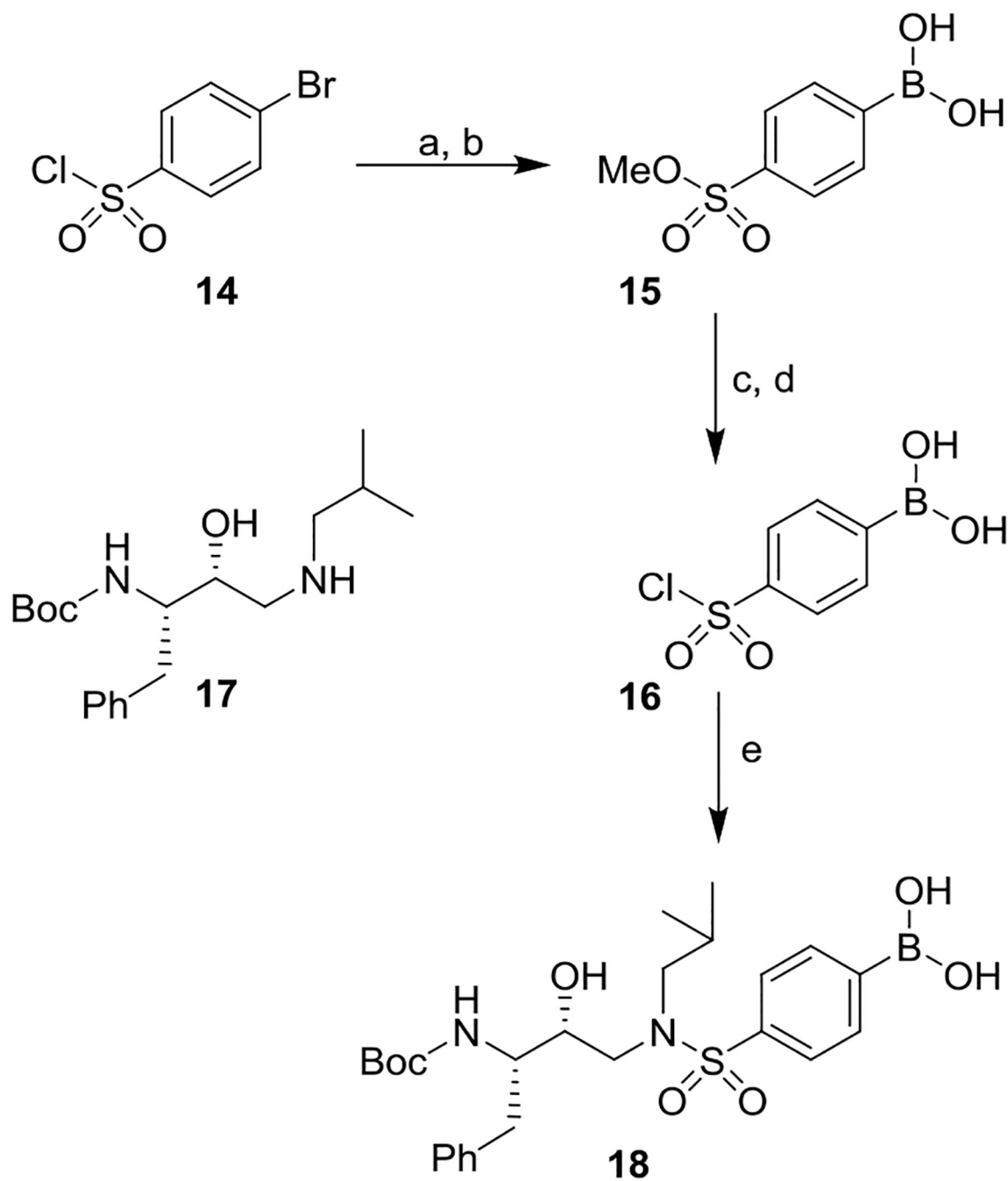


Figure 3.

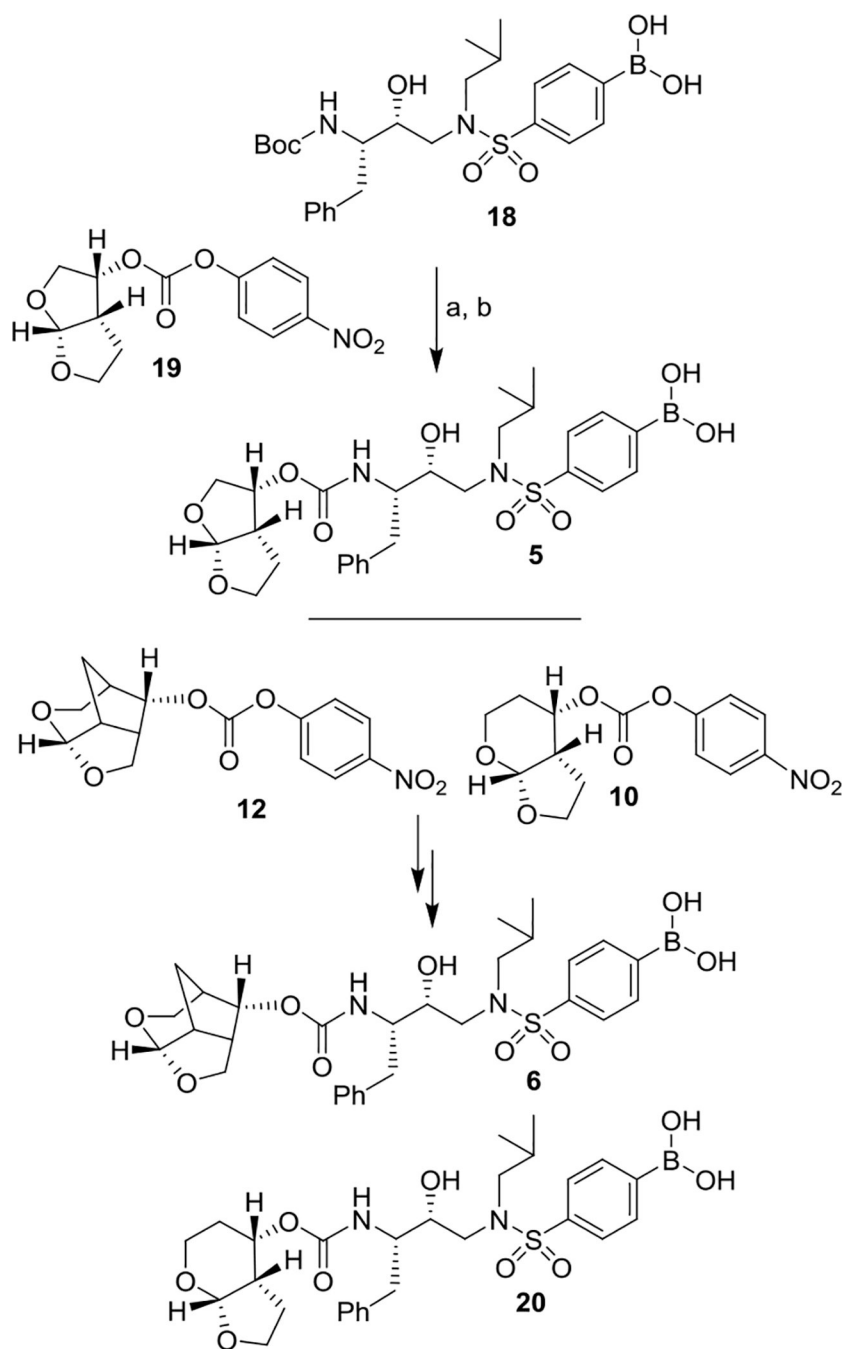
A. The X-ray structure of inhibitor **6**-bound HIV-1 protease (carbon atoms, turquoise; PDB ID: 6U7O). **B.** The X-ray structure of inhibitor **20**-bound HIV-1 protease (carbon atoms, orange; PDB ID: 6U7P). The major orientations of the inhibitors are shown. All water molecules are red spheres, the hydrogen bonds are shown by dotted lines and bond lengths are shown in the S2'-subsite.

**Scheme 1.**

Synthesis of PIs **11**, and **13**. Reagents and chemicals. (a) K_2CO_3 , MeOH, 23 °C, 30 min; (b) $NaClO_2$, 2-methyl-2-butene, NaH_2PO_4 , $tBuOH-H_2O$, 23 °C, 3 h (86% for 2-steps); (c) TFA, CH_2Cl_2 , 0 °C to 23 °C, 3 h; (d) **10**, DIPEA, CH_3CN , 23 °C, 12 d (37–80% for 2-steps).

**Scheme 2.**

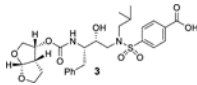
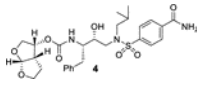
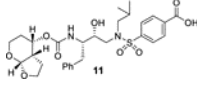
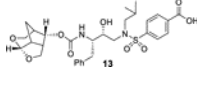
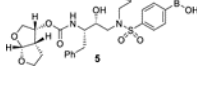
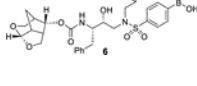
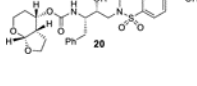
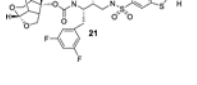
Synthesis of boronic acid derivative **18**. Reagents and chemicals. (a) NaOMe, MeOH, 0 °C to 23 °C, 12 h (62%); (b) nBuLi, THF, -78 °C, B(OMe)₃, 30 min (45%); (c) Et₃N, MeOH, 60 °C for 24 h; (d) SOCl₂, 80 °C for 24 h (89% for 2-steps); (e) Et₃N, CH₂Cl₂, 0 °C to 23 °C, 1 h (82%).

**Scheme 3.**

Synthesis of PIIs. Reagents and chemicals. (a) TFA, CH₂Cl₂, 0 °C, 30 min; (b) carbonate **19**, DIPEA, CH₃CN, 23 °C, 10 d, (47% yield for 2-steps).

Table 1.

Structures and activity of carboxylic and boronic acid containing inhibitors.

Entry	Inhibitor	K_i (pM) ^a	IC_{50} (nM) ^c
1		12.9	>1000
2		8.9	93
3		7.6	>1000
4		3.2	>1000
5		0.5 ^b	48.9
6		15.5	37.7
7		2.1	120
8		14	0.017

^a K_i values represents at least 5 data points. Standard error in all cases was less than 7%. Darunavir (DRV) exhibited K_i = 16 pM.^b reported value.^cValues are means of at least three experiments in MT-2 cells. Standard error in all cases was less than 5%. DRV exhibited IC_{50} = 1.6 nM.

Table 2.

Antiviral activity of novel compounds against highly DRV-resistant HIV-1 variants.

	Mean IC ₅₀ in nM (fold-change)				
	LPV	1 (DRV)	5	6	21 (GRL-14213)
cHIV _{LAI} ^{WT}	13	3.2	48.9	37.7	0.017
HIV _{DRV} ^R _{p20}	>1000 (>77)	525.8 (164)	219.3 (4)	71.2 (2)	0.0024
HIV _{DRV} ^R _{p30}	>1000 (>77)	601 (187)	946.4 (19)	532.3 (14)	0.14
HIV _{DRV} ^R _{p51}	>1000 (>77)	5429.7 (1696)	>1000	>1000	1.3

Numbers in parentheses represent fold changes in IC₅₀s for each isolate compared to the IC₅₀s for wild-type cHIV_{LAI}^{WT}. All assays were conducted in triplicate, and the data shown represent mean values (±1 standard deviation) derived from the results of three independent experiments. DRV, Darunavir; LPV, Lopinavir.